

## Advanced treatment of secondary effluent by the integration of heterogeneous catalytic ozonation and biological aerated filter

Xinghao Liu<sup>a,b</sup>, Zhaoguang Yang<sup>a,b</sup>, Jiayun Peng<sup>c</sup>, Leilei Chen<sup>a,b</sup>, Ying Yang<sup>a,b</sup>, Haipu Li<sup>a,b</sup> and Liqun Yang<sup>c,\*</sup>

<sup>a</sup> Center for Environment and Water Resource, College of Chemistry and Chemical Engineering, Central South University, Changsha 410083, China

<sup>b</sup> Key Laboratory of Hunan Province for Water Environment and Agriculture Product Safety, Changsha 410083, China

<sup>c</sup> Logistics Support Department of the Xiangya Hospital, Central South University, Changsha 410083, China

\*Corresponding author. E-mail: yangliqun@xiangya.com.cn

### ABSTRACT

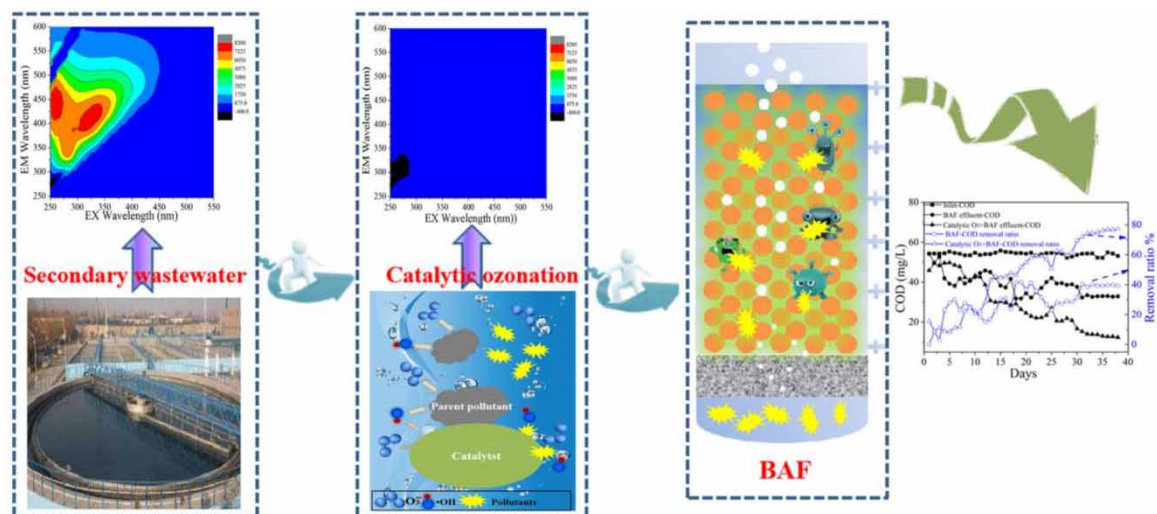
The advanced treatment of secondary effluents was investigated by employing heterogeneous catalytic ozonation integrated with a biological aerated filter (BAF) process. The results indicated that catalytic ozonation with the prepared catalyst ( $Mn_xCu_yO_z/\gamma-Fe_2O_3$ ) significantly enhanced the performance of pollutant removal and broke up macromolecules into molecular substances by the generated hydroxyl radicals. These molecular substances were easily absorbed by microorganisms in the microbial membrane reactor. In the BAF process, chemical oxygen demand (COD) (chemical oxygen demand) decreased from 54.26 to 32.56 mg/L, while in catalytic ozonation coupled with the BAF, COD could be reduced to 14.65 mg/L (removal ratio 73%). Under the same condition,  $NH_4^+-N$  decreased from 77.43 to 22.69 mg/L and 15.73 mg/L (removal ratio 70%) in the BAF and the catalytic ozonation coupled with BAF, respectively. In addition, the model that highly correlated influent COD to effluent COD and reactor height for filler could predict the removal ratio of COD of the BAF system. Based on the microbial community analysis, ozone in the solution had a certain screening effect on microorganisms, which helped to better adapt to the ozone-containing environment. Therefore, the integrated process with its efficient, economic, and sustainable advantages was suitable for the advanced treatment of secondary effluents.

**Key words:** BAF, biodegradability, empirical model, microbial community

### HIGHLIGHTS

- The biodegradability of municipal wastewater was improved after ozonation.
- The COD at different BAF heights as a function of influent COD was established.
- Catalytic ozonation coupled with BAF for advanced treatment of wastewater was feasible.

## GRAPHICAL ABSTRACT



## 1. INTRODUCTION

In the municipal wastewater treatment plant, the conventional treatment processes, e.g. the mainstream activated sludge anaerobic–anoxic–oxic ( $A^2/O$ ) and sequencing batch reactor (SBR) systems, are commonly used (Su *et al.* 2021; Singh *et al.* 2022). However, limited by the biodegradability of pollutants, there are still some refractory or toxic organic pollutants that remained in the biological effluent, including pesticides, antibiotics, sunscreen, etc. (Wu *et al.* 2018; Shreve & Brennan 2019; Tang *et al.* 2022). The pollutants that cannot be effectively removed are discharged into the environment directly with sewage. Although they usually exist in the water ecosystem at light concentration, long-term exposure will damage the micro-ecosystem and cause the presence of drug-resistant pathogens. Therefore, the advanced treatment of secondary effluent has received extensive attention (Gonder *et al.* 2020; Satayavibul & Ratanatamskul 2021).

Nowadays, advanced oxidation technologies (AOTs) have been intensely investigated and often used for advanced sewage treatment, e.g. ozonation, Fenton/Fenton-like reactions, photo-catalysis, and the activated persulfate method (Chavez *et al.* 2020; Su *et al.* 2021; Tang *et al.* 2021b). Among these advanced sewage treatment methods, ozonation is considered a promising advanced technology, because it saves equipment space, produces less sludge, reacts faster, and does not require extra energy or soluble chemicals. The catalytic ozonation can improve the biodegradability of wastewater, reduce the refractory pollutants and also partly decrease chemical oxygen demand (COD). For example, Zhang *et al.* (2014) found that biochemical oxygen demand ( $BOD_5$ )/COD of coking wastewater could increase from 0.09 to 0.43, indicating that the biodegradability of the wastewater was improved, and the residual refractory pollutants with large molecules could be transformed into smaller ones after catalytic ozonation treatment (Liu *et al.* 2021, 2022a). Qiu *et al.* (2022) used the catalytic ozonation system to treat refractory organics from secondary effluent, and the different pollutants had different reaction rates with ozone/hydroxyl radicals ( $\cdot OH$ ). Also, these products were difficult to be completely mineralized in a short period of time (Chen *et al.* 2022; Wang *et al.* 2022). Excitedly, the generated small molecules could be easily removed by the biological treatment process. The biological aerated filter (BAF), as an alternative fixed-film process, had been widely used to treat various wastewater, including municipal and industrial wastewaters (Vatankhah *et al.* 2019; Li *et al.* 2020), due to its excellent characteristics, involving a small footprint, simple operation and maintenance, higher biomass concentration, less sludge production, and effective pollutants removal (Zhou & Xu 2020). Many studies investigated the pollutants removal ratios, operational parameters optimization, and microbial community structures for established BAF systems (Ren *et al.* 2019; Xiang *et al.* 2021). BAF was with a vertical column, thus the bio-community could readily adapt to the different levels of dissolved oxygen (DO) and/or renewable water quality. Therefore, an integration of catalytic ozonation and the BAF system would be a satisfactory method for enhancing the removal capacity of pollutants. Also, the BAF structures and types of filter media were related to installation costs and removal ratios of pollutants (Xiang *et al.* 2021). BAF with various structures and different types of filter media had been prepared, and it was impractical and cost-prohibitive to evaluate their performance individually (Xiang *et al.*

2021; Nikoonahad *et al.* 2022). If there was a way to relate influent COD to effluent COD and reactor height for specific media, it would be critical for providing important information for the design and optimization of water treatment processes towards cost-effectiveness.

In this study, the effects of catalytic ozonation coupled with up-flow BAF on the advanced treatment of secondary effluent were investigated. The influences of catalytic ozonation on secondary effluent treatment are described in detail, including water quality parameters (e.g. COD,  $UV_{254}$ ,  $NH_4^+-N$ , and total organic carbon (TOC) and economic analysis. Importantly, the COD removal kinetics behavior as a function of influent COD concentration in the BAF was investigated. This study provides a reference for the advanced treatment of secondary effluents for practical purposes.

## 2. MATERIALS AND METHODS

### 2.1. Materials

The raw water sample was the secondary effluent obtained from a conventional activated sludge system (anaerobic–anoxic–oxic ( $A^2/O$ ) process) in a municipal wastewater treatment plant in Changsha, China. The removal of soluble substances was deeply researched, therefore, to avoid the negative effect of suspended solid (SS), the raw water was filtered by  $0.45\ \mu\text{m}$  glass fiber film in advance. The water characteristics are shown in Table 1.

### 2.2. Experimental setup

The experimental setup was composed of a catalytic ozonation system and a BAF system (Figure 1). The catalytic ozonation system mainly consisted of the ozone generator, ozone catalytic reactor, and exhaust gas treatment device, and the parameters of the ozone catalytic reactor were shown in the previous study (Liu *et al.* 2021). For the BAF system, the BAF reactor was made of plexiglass with an inner diameter of 60 mm and a height of 2,000 mm with the micro-porous air diffuser fixed at the bottom of the BAF column. The sampling port interval was about 150 mm. The filter material was a homemade particle ceramsite with a diameter of about 7–9 mm, and the filling height was approximately 1,200 mm.

**Table 1** | The raw water characteristics of secondary effluent

Parameter	COD (mg/L)	TOC (mg/L)	TNS (mg/L)	$NH_4^+-N$ (mg/L)	$UV_{254}$ (Abs)	pH
Secondary effluent	52.2–55.3	4.15–4.34	–	74.3–77.8	0.13–0.16	7.2–7.8

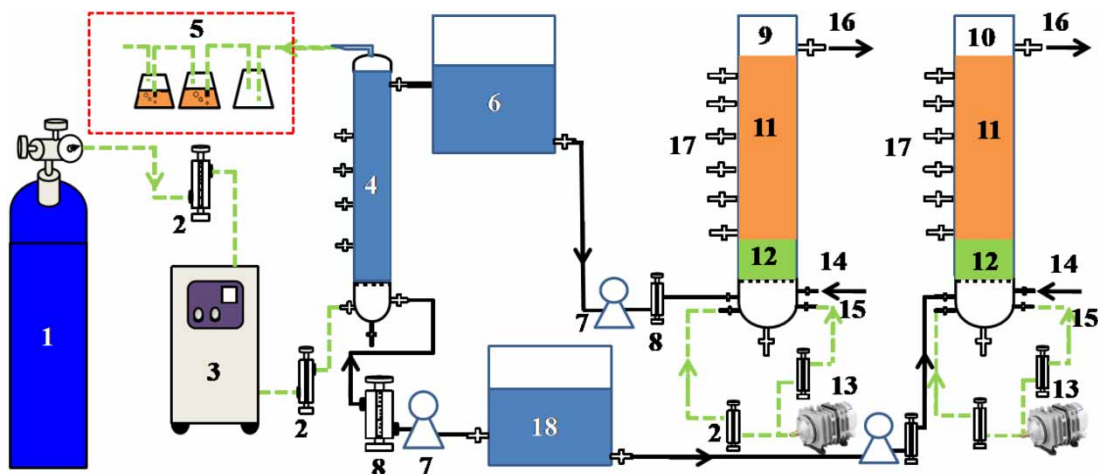


**Figure 1** | The schematic diagram of experiment setup: (1) oxygen; (2) gas flowmeter; (3) ozone generator; (4) ozone reactor; (5) exhaust gas treatment device; (6) middle tank; (7) peristaltic pump; (8) fluid flowmeter; (9) catalytic ozone baf column; (10) baf column; (11) ceramsite; (12) cobblestone; (13) air pump; (14) backwash water; (15) backwash gas; (16) backwashing outlet; (17) sample port; and (18) wastewater tank.

### 2.3. Operating parameters

The catalytic ozonation reactor held 1 L of reaction solution with 0.5 g/L catalysts ( $\text{Mn}_x\text{Cu}_y\text{O}_z/\gamma\text{-Fe}_2\text{O}_3$ ), which had been proven to possess excellent catalytic activity against ozone by a previous study (Liu *et al.* 2022a). The synthesis method of  $\text{Mn}_x\text{Cu}_y\text{O}_z/\gamma\text{-Fe}_2\text{O}_3$  is shown in Supplementary Materials, Text S1. Furthermore, the characteristics including crystal structure and surface morphology are supplied in Text S2. The generated ozone via the ozone generator entered the reaction solution through the porous aeration plate and the gas flow rate and ozone dosage were about 200 mL/min and 10 mg/L, respectively. For the BAF reactor, the ozone-pretreated secondary effluent/secondary effluent entered from the bottom of the up-flow BAF, which mixed well with the air generated by the micro-porous air diffuser at the bottom of the column. The effective volume and the hydraulic retention time (HRT) were about 2 L and 2 h, respectively. The flow rate of air was controlled according to the requirement of a gas-water ratio of 3:1.

### 2.4. Analysis methods

The concentrations of water characteristics including COD, BOD, and  $\text{NH}_4^+\text{-N}$  were detected via the standard methods (APHA 2015). The DO and pH were routinely monitored by a DO meter (HQ30d, HACH, USA) and pH meter (pHSJ-3F, Leici, China), respectively. The TOC was measured by the TOC analyzer (TOC-V<sub>CPH</sub>, Shimadzu, Japan). The UV<sub>254</sub> was detected by a UV-visible spectrophotometer (TU-1810, PERSEE, China). In addition, the soluble organic matter was measured by a three-dimensional fluorescence spectrometer (HORIBA, Canada). The concentrations of ozone in the gas phase and solution were determined by iodometry and indigo methods, respectively (Liu *et al.* 2018).

Biofilm samples were detached from the surface of ceramsite in the BAF reactor. The samples were obtained from the single BAF (Sample 1) and catalytic ozonation coupled BAF (Sample 2) systems. DNA was extracted using a PowerBiofilm™ DNA Isolation Kit for Biofilm (Mo Bio, Carlsbad, CA, USA) and stored at  $-80^\circ\text{C}$ . The microbial community structure was further analyzed with high-throughput sequencing technology, using Illumina Hiseq 2000 from the Shanghai Meiji Biomedical Technology Co., Ltd (Shanghai, China).

### 2.5. The model for COD removal kinetics in BAF

As for the model of relating influent COD to effluent COD and reactor height for homemade ceramsite, the pretreated wastewater was assumed to pass through the packing in a plug flow and the removal of COD would conform to pseudo-first-order kinetics in BAF. The COD removal pseudo-first-order kinetics is shown in the following Equation (1) (Mann & Stephenson 1997):

$$\frac{dC}{dt} = -k_1XC \quad (1)$$

where  $dC/dt$  is the COD removal rate,  $k_1$  is the rate constant, and  $C$  is the COD concentration (mg/L).  $X$  is the microbial biomass concentration (mg/L), and  $X$  is related to the medium surface property and type, which are generally expressed as a function of the specific surface area of the medium,  $X=f(A)$ . Equation (1) can be transformed into the following equations:

$$\frac{dC}{dt} = -k_1f(A)C = -K_1C \quad (2)$$

$$\ln \frac{C}{C_i} = -K_1t \quad (3)$$

where  $t$  is the mean retention time (h), which can be expressed as the following equation (Mann & Stephenson 1997):

$$t = \frac{k}{B_W} \quad (4)$$

where  $k'$  is the biomass constant, and  $B_W$  is the volumetric loading, which can be expressed as the following equation:

$$B_W = \frac{QC_i}{HA} \quad (5)$$

where  $Q$  is the volumetric flow rate ( $\text{m}^3/\text{h}$ ), and  $A$  is the cross-sectional area of the reactor ( $\text{m}^2$ ). Based on Equations (4) and (5), Equation (3) can be expressed as the following equation:

$$\ln \frac{C}{C_i} = -\frac{K_1 k' A}{QC_i} H = -\frac{k^* A}{QC_i^m} H \quad (6)$$

where  $m$  is a constant dependent on the medium type, and  $k^* = K_1 k'$  (the overall process constant). The  $k^*$  represents the overall COD removal performance along the height of the BAF system at the influent COD concentration. The higher the  $k^*$  value is, the higher the COD removal ratio is. In addition, the  $K = k^* A / QC_i^m$ , thus Equation (6) can be simplified to the following equation:

$$\ln \frac{C}{C_i} = -KH \quad (7)$$

By plotting  $\ln(C/C_i)$  against  $H$ , the slope  $K$  can be obtained for different values of  $C_i$ . The slope  $m$  and the intercept  $\ln k^*$  can be determined from the plot of  $\ln(KQ/A)$  against  $\ln(C_i)$ , respectively.

### 3. RESULTS AND DISCUSSION

#### 3.1. The catalytic performance for wastewater treatment

The effects of catalytic ozonation on secondary effluent were investigated. As shown in Figure 2(a) and 2(b), the removal ratios of COD and TOC increased with increasing treatment times, but the removal ratios were low, indicating that the COD and TOC were difficult to remove in a short period. In the ozonation system, the removal ratio of COD was about 6.5% in 30 min, and the TOC removal ratio was 5.3% under the same condition. The removal ratios of COD and TOC in 30 min were close to those in 20 min. In the catalytic ozonation system, the removal ratios of COD and TOC were about 17.1 and 11.5%, respectively, in 20 min. The above results showed that ozonation could remove parts of COD and TOC, and the performance of catalytic ozonation was better than that of ozonation. The ozone could be quickly decomposed to generate strong oxidative and no selective  $\cdot\text{OH}$  in the presence of the catalyst (Chen & Wang 2021; Liu *et al.* 2022b), which facilitated the removal of organic matter in the solution. The  $\text{UV}_{254}$  could be well removed by ozonation and catalytic ozonation (Figure 2(c)). It had an obvious removal rate in the first 5 min, but the removal rate gradually decreased after 5 min. In the initial stage, the ozone and generated  $\cdot\text{OH}$  could quickly attack the humic acid and organic matter with structures  $\text{C}=\text{C}$  and  $\text{C}=\text{O}$ . As the reaction progressed, the structures of these substances were destroyed, which led to a reduced removal ratio. Also, the removal ratio in the catalytic ozonation system was higher than that in the single ozonation system, indirectly indicating that the oxidative capacity of  $\cdot\text{OH}$  was higher than that of ozone. As for the  $\text{NH}_4^+\text{-N}$  (Figure 2(d)), ozonation and catalytic ozonation could remove a certain amount of it, but the effect was not obvious. As known, the removal of  $\text{NH}_4^+\text{-N}$  relied mainly on microorganisms (Ushiki *et al.* 2018), and the  $\text{NH}_4^+\text{-N}$  did not change significantly after ozonation or catalytic ozonation. Based on the above analysis, catalytic ozonation was an effective pretreatment method.

Also, the organic matter in the solution was detected by 3D fluorescence spectroscopy. Before detection of it, the catalyst was separated from the solution by a magnet due to its magnetic properties. As shown in Figure 3(a), there were three absorption peaks in the raw water and they were located at  $Ex/Em = 250\text{--}260/410\text{--}470$ ,  $270\text{--}280/340\text{--}350$ , and  $310\text{--}350/375\text{--}440$  nm, which correspond to humic substances, protein substances, and fulvic acids, respectively (Parlanti *et al.* 2000). Within 30 min of the reaction (Figure 3(b)–(d)), the fluorescence intensities were decreased with increasing the treatment times. The decreasing trends of fluorescence intensities were consistent with the results of  $\text{UV}_{254}$ . To further analyze the changes in substances, the maximum fluorescence intensities were modified (Fig. S3). The intensity of the fluorescence peaks (humic acid and fulvic acid) in the 30 min treated solution decreased to 500 compared to that of 8200 in raw water,



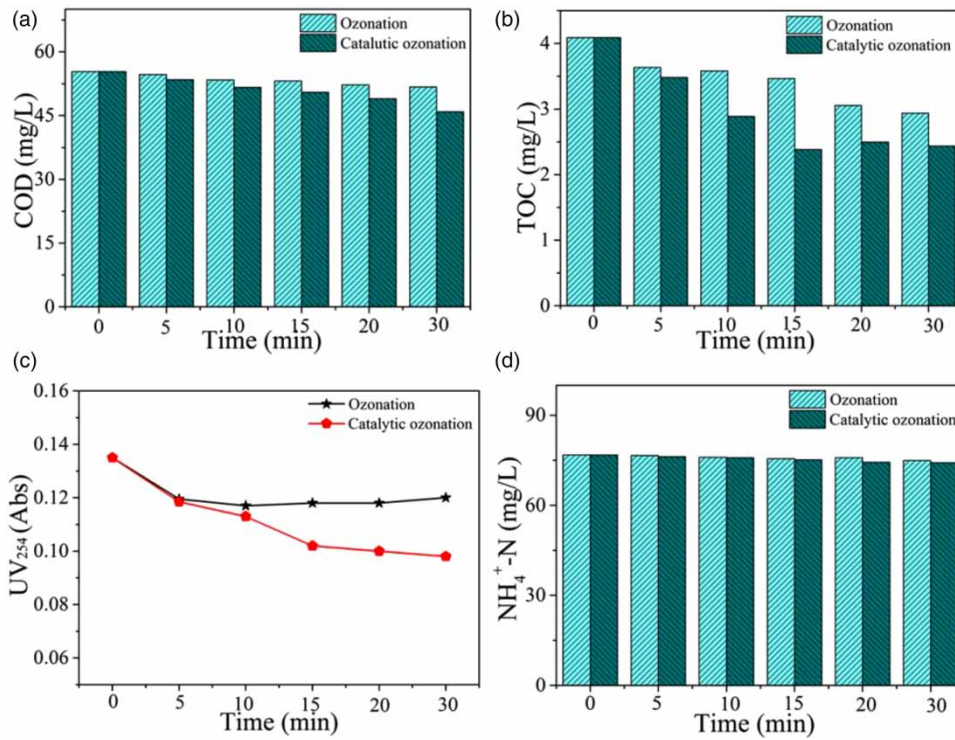


**Figure 2** | The changes of (a) COD, (b) TOC, (c) UV<sub>254</sub>, and (d) NH<sub>4</sub><sup>+</sup>-N in the ozonation and catalytic ozonation systems. Conditions: 1 L reaction solution, 0.5 g/L Mn<sub>x</sub>Cu<sub>y</sub>O<sub>z</sub>/γ-Fe<sub>2</sub>O<sub>3</sub>, pH 7.3, ozone dosage 200 mL/min, and 10 mg/L.

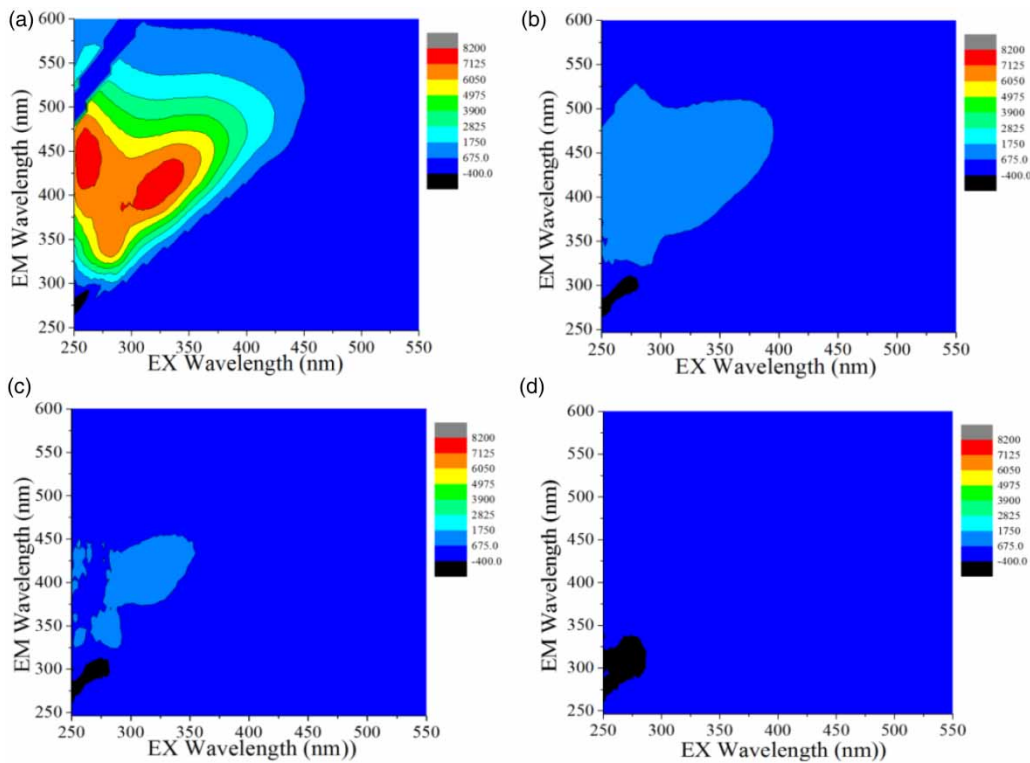


**Figure 3** | Three-dimensional fluorescence in secondary effluent after catalytic ozonation, (a) raw water, (b) 10 min, (c) 20 min, and (d) 30 min.

and the fluorescence peak of protein substances disappeared. The above results indicated that the structures of humic substances, protein substances, and fulvic acids could be well destroyed by catalytic ozonation.

### 3.2. Economic operation analysis for the ozonation system

The economic operation was an important criterion for judging whether a technology could be widely promoted. In this study, the economic analysis model was used to evaluate the economics of catalytic ozonation for the pollutants removal in secondary effluent (Vinoth Kumar *et al.* 2020). The model mainly relied on the equivalent relationship between the ozone dosage and the removal ratios of the pollution index, in other words, the indicators of electricity and specific pollutant degradation kinetic constants, as shown in Equation (8). In this study, the rated power of the ozone generator and the volume of the treatment solution were 0.18 kW and 1 L, respectively. The COD was a parameter indicator and the degradation kinetics are supplied in Text S3. Based on the calculation,  $k$  was 0.8148 and 2.0946  $\text{h}^{-1}$  in ozonation and catalytic ozonation systems, respectively. The electrical energy per order (EE/O) was 110.47 and 42.97 for the COD removal in ozonation and catalytic ozonation systems, respectively. The EE/O value of COD removal in the catalytic ozonation system was 2.57 times higher than that in the ozonation system, indicating that the addition of catalyst reduced energy consumption and improved the economy of the pre-oxidized treatment of secondary effluent. Therefore, catalytic ozonation was selected as the pretreatment technology for the secondary effluent:

$$EE/O = \frac{Pt}{V \cdot k} \quad (8)$$

where  $P$  (kW) represents the operating power of the ozone generator;  $V$  (L) is the volume of the treatment solution;  $k$  ( $\text{h}^{-1}$ ) is the degradation kinetic constant of the pollution index.

### 3.3. Kinetic behavior as a function of influent COD concentration in BAF

As known, the removal of COD via BAF system was related to BAF construction and filler media types (Bao *et al.* 2016). In this study, the BAF reactor with homemade filler ceramsite was used to analyze the COD removal kinetic model. Based on influent COD concentrations of 0.05, 0.1, 0.2, and 0.4  $\text{kg}/\text{m}^3$  in BAF, the COD concentrations at different heights (0.3, 0.6, and 0.9 m) were detected. Within the designed height of the BAF, the  $-\ln(C/C_i)$  had a good linear relationship with the designed height ( $H$ ), as shown in Figure 4(a). According to the linear fit, the reaction kinetic constants could be obtained, and they were  $K = 0.480, 0.180, 0.154,$  and  $0.120$  for the influent COD concentrations of 0.05, 0.1, 0.2, and 0.4  $\text{kg}/\text{m}^3$ , respectively. Furthermore, based on the  $K = k^*A/QC_i^m$ , the linear regression of  $-\ln(KQ/A)$  with  $\ln(C_i)$  could get the values of  $m$  and  $\ln(k^*)$ , and they were 0.622 and 3.742, respectively (Figure 4(b)). The values of  $m$  and  $\ln(k^*)$  were introduced into Equation (6) to obtain Equation (9). Therefore, the removal ratio of COD could be predicted via Equation (9) in this established BAF. Mann & Stephenson (1997) reported that the values of  $k^*$  and  $m$  ranged from 33 to 55 and from 0.92 to 1.13, respectively,

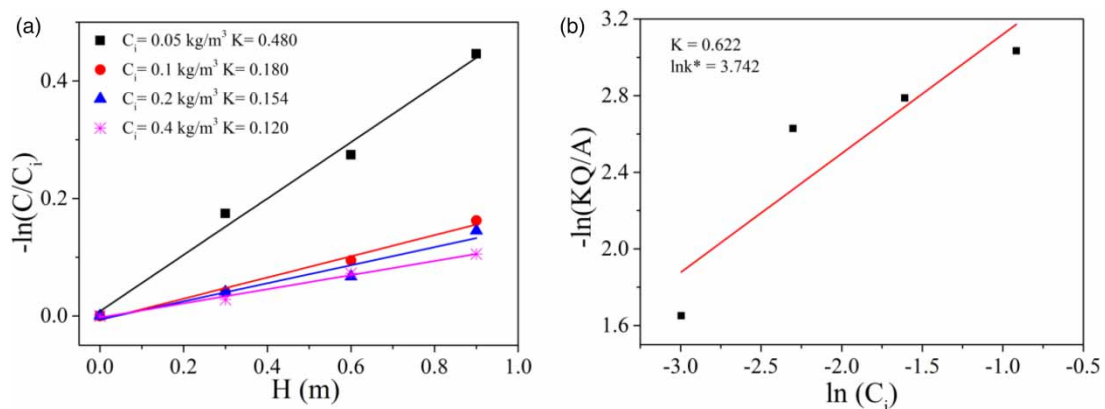


**Figure 4** | (a) The relationship curve between  $-\ln(C/C_i)$  and  $H$  of BAF height; (b) the linear fitting of  $-\ln(KQ/A)$  against  $\ln(C_i)$ .

and the difference in their values was mainly due to the difference in wastewater characteristics:

$$\ln \frac{C}{C_i} = -\frac{k^* A}{QC_i^m} H = -\frac{42.169 \times 0.06}{QC_i^{0.622}} H = -\frac{2.53}{QC_i^{0.622}} H \quad (9)$$

### 3.4. The performance of catalytic ozonation coupled with BAF

To evaluate the performance of the constructed catalytic ozonation coupled with the BAF system for secondary effluent treatment, the water quality parameters including COD,  $\text{NH}_4^+\text{-N}$ , TOC,  $\text{UV}_{254}$ , pH, and DO were analyzed (Table 1). The influent volume, HRT, and gas-liquid flow rate ratio were about 16.7 mL/min, 2 h, and 3:1, respectively. Figure 5(a) shows the change in COD. In the BAF system, the COD of the solution decreased from 54.26 to 32.56 mg/L, and the highest removal ratio of COD was just about 40% because the biodegradability of the secondary effluent was low ( $\text{BOD}_5/\text{COD} = 0.00163$ ). While in the catalytic ozonation coupled with the BAF system, the COD of the solution decreased from 54.26 to 14.65 mg/L and the COD removal ratio could reach 73%, because the catalytic ozonation could significantly improve the biodegradability of secondary effluent, and the value of  $\text{BOD}_5/\text{COD}$  was 42.1 times that for ozonation. However, during initial operation, the effluent COD in the BAF system was slightly lower than that in the catalytic ozonation coupled with the BAF system, because the residual ozone in the solution could lead to a shedding of biofilms (Fu *et al.* 2021). Over time, the microorganisms gradually adapted to the water environment in the presence of ozone, and a stable biofilm system was formed on the surface of ceramsite, which could accelerate COD removal (Wu *et al.* 2015). As a comparison, in the study by Wang *et al.* (2008), a BAF system with clay-based media was employed to treat the domestic wastewater, and the COD removal ratio decreased continuously and stabilized for 25% after two cultural weeks. In addition, Zhang *et al.* (2014) used BAF with ceramic media to treat the coking wastewater, and the COD removal ratio was maintained at about 30%, which was attributed to the low organic loading from the coking wastewater effluent. The above results indicated that the single BAF was hard to

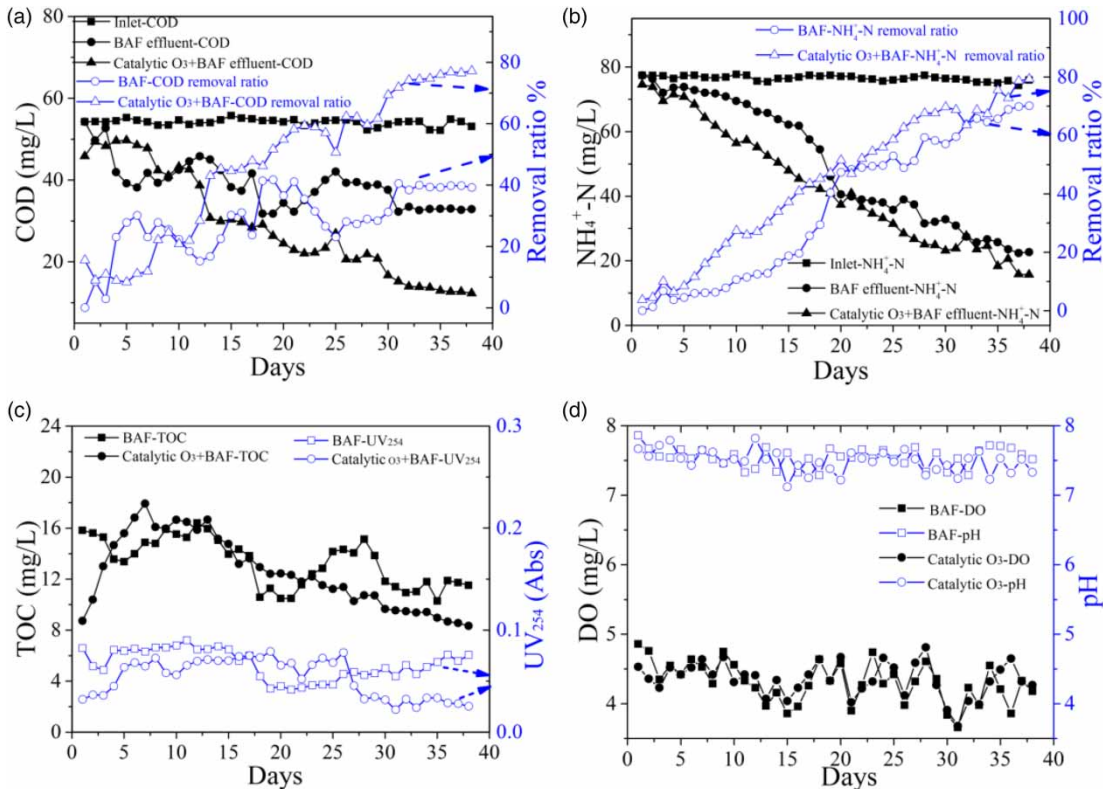


**Figure 5** | Changes of water quality parameters during operation of BAF and catalytic ozonation coupled with BAF, (a) COD, (b)  $\text{NH}_4^+\text{-N}$ , (c) TOC and  $\text{UV}_{254}$ , and (d) pH and DO.



remove the COD due to the low organics loading of wastewater. In addition, the catalytic ozonation could improve the organics loading, which was beneficial to enhance COD removal.

Figure 5(b) displays the variation of  $\text{NH}_4^+\text{-N}$  with operating time. In the first 30 days, the removal ratio of  $\text{NH}_4^+\text{-N}$  fluctuated with the increasing operation time, while, after 30 days, the removal ratio remained relatively stable. In the process of the established BAF,  $\text{NH}_4^+\text{-N}$  decreased from 77.43 to 22.69 mg/L with a removal ratio of about 70%. In the catalytic ozonation coupled with the BAF system, at the same condition, the  $\text{NH}_4^+\text{-N}$  decreased from 77.43 to 15.73 mg/L in the catalytic ozonation coupled with the BAF system and the removal ratio could reach about 78%. In the initial stage, the nitrifying and denitrifying bacteria had an adaptative process to water quality with residual ozone (Zhou *et al.* 2019). With longer operation times, the bacteria gradually accumulated and enriched on the surface of the ceramsite to form a stable biofilm, which facilitated the removal of  $\text{NH}_4^+\text{-N}$ . According to a review study by Jin *et al.* (2023), the microorganisms with significant degradability were in the BAF system. Most of the denitrifying bacteria were nitrite-oxidizing bacteria and ammonia-oxidizing bacteria. In detail, in the aerobic environment, the  $\text{NH}_4^+\text{-N}$  was oxidized to  $\text{NO}_2^-$  by the ammonia-oxidizing bacteria, including *Nitrosomonas*, *Nitrosococcus*, *Nitrosolobus*, and *Nitrosovibrio*, etc. (Ushiki *et al.* 2018). The  $\text{NO}_2^-$  was further oxidized to generate the  $\text{NO}_3^-$  by the nitrite-oxidizing bacteria, including *Nitrobacter*, *Nitrospina*, *Nitrococcus*, etc. (Friedrich *et al.* 2020). At last, the generated  $\text{NO}_3^-$  was reduced to  $\text{N}_2$  under the anoxic conditions by the heterotrophic denitrifying bacteria (Daims *et al.* 2015). Therefore, the  $\text{NH}_4^+\text{-N}$  in the solution was supposed to be transformed into  $\text{N}_2$  in this study. However, the study by Bao *et al.* (2016) used commercially available ceramsite as the filter media for BAF to remove  $\text{NH}_4^+\text{-N}$  and the removal ratio was about 67.29%. In this study, the BAF with homemade ceramsite media could remove 70%  $\text{NH}_4^+\text{-N}$ . Therefore, the homemade sludge base ceramsite might be suitable for use as filter media for the simultaneous removal of  $\text{NH}_4^+\text{-N}$  and COD.

The TOC and  $\text{UV}_{254}$  of the solution are shown in Figure 5(c). TOC showed a trend of decreasing volatility. In the catalytic ozonation coupled with the BAF system, the TOC had slightly increased, which was caused by the shedding of part of the biofilm in the initial stage. At last, the TOC removal ratio tended to stabilize. The changing trend was consistent with that of the COD. In addition, the  $\text{UV}_{254}$  was also volatile in both systems (0.04–0.085 Abs in BAF and 0.02–0.075 Abs in catalytic ozonation coupled with BAF). The pH and DO had important influences on the growth of microorganisms. Figure 5(d) shows the change in pH and DO during the operation. The pH of the solution was about 7–8, and the DO was about 4–5 mg/L. The above conditions were suitable for the growth of microbial films, which could promote the removal of pollutants by microorganisms (Tang *et al.* 2021a).

To evaluate the removal effect of the established integration of heterogeneous catalytic ozonation and the BAF system on pollutants, Table S1 summarizes the system performance of BAF combined with other processes. Zhang *et al.* (2014) used the ozonation-coupled BAF system to treat the bio-treated coking wastewater with 59 and 76% removal of COD and  $\text{NH}_4^+\text{-N}$ , respectively. Farabegoli *et al.* (2009) adopted the chemical precipitation coupled BAF system to dispose of domestic sewage with 33, 96, and 66% removal of COD,  $\text{NH}_4^+\text{-N}$ , and total suspended solid (TSS), respectively. In addition, Xu *et al.* (2015) used heterogeneous Fenton oxidation (HFO) with an anoxic moving bed biofilm reactor to treat the biologically pretreated coal gasification wastewater, and the removal ratios of COD, total phenols and total nitrogen (TN) were 82, 83, and 85%, respectively. In this study, we used the integration of heterogeneous catalytic ozonation and BAF to dispose of the secondary effluent from the waste water treatment plant (WWTP), and the removal ratios of COD and  $\text{NH}_4^+\text{-N}$  were 73 and 70%, respectively. Based on these results, it would be a trend to combine biofilters with advanced oxidation processes to improve pollutant degradation efficiency with low energy consumption were a tendency. The BAF treatment was once very popular due to its stable discharge for high standards of effluent.

### 3.5. Microbial community

To analyze the microbial community variation before and after ozone treatment, high-throughput sequencing technology was used. The dilution curves for microbial high-throughput sequencing are shown in Figure 6(a). As the number of sequencing increased, the dilution curve became flatter, indicating that fewer new operational taxonomic units (OTUs) were added and the amount of sequencing was more reasonable (Zhou & Xu 2019). When the sequencing amount was 30120, the OTUs of biofilms were 760 and 499 in the BAF and catalytic ozonation coupled BAF systems, respectively. The results of the biological sequence could reflect the vast majority of bacterial biological information, hence it could be used for subsequent analysis.

The Shannon, Simpson, and Chao1 index could all reflect the microbial diversity variation (Fu *et al.* 2021). The high Shannon index indicated rich community diversity, and the low Simpson index indicated rich community diversity (Ding *et al.*

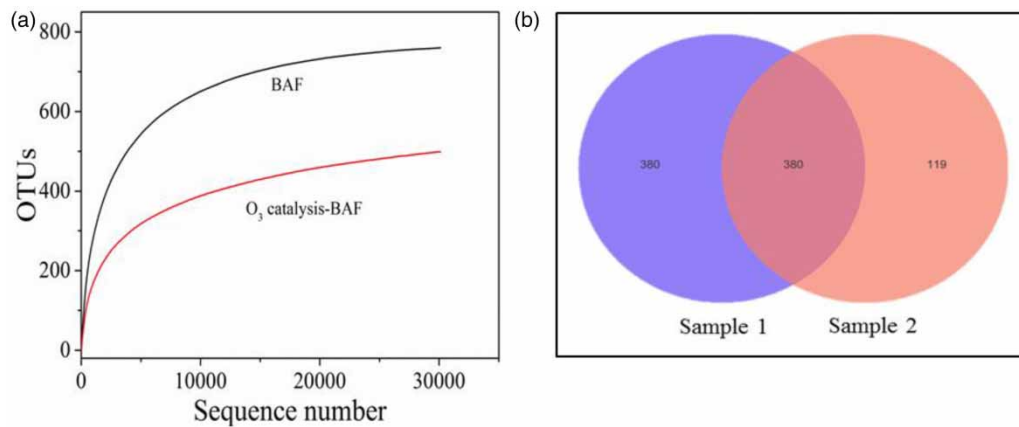


**Figure 6** | (a) Rarefaction curves of the BAF biofilms, (b) the Venn diagram of the OTUs numbers of the BAF biofilms (BAF-Sample 1, Catalytic ozonation/BAF-Sample 2).

2018). The Chao1 index was the same as OTUs, they all could account for changing species in community abundance and biofilms. As shown in Table 2, the Shannon, Simpson, and Chao1 indices of the microbial film in BAF were 5.2037, 0.0178, and 772.176, respectively, and the indices were 4.2132, 0.0368, and 576.782, respectively, in catalytic ozonation coupled BAF. These indices indicated that the biofilms in BAF exhibited high community richness, while the biofilms in catalytic ozonation coupled BAF had the advantage of community diversity. The residual ozone in the solution could screen microorganisms and the available carbon sources promoted thriving microbial growth.

Figure 6(b) shows the Venn diagram of OTUs for Samples 1 and 2. The common OTUs between Samples 1 and 2 were 380, while the proprietary OTUs were 380 and 119, respectively. The differences in the microbial communities in Samples 1 and 2 were small. The reason for this difference might be the screening effect of the residual ozone in the sewage on the microorganisms (Zhang *et al.* 2018).

All valid sequences were classified and analyzed except for the analysis of OTUs in this study, and a total of 29 phyla, 63 classes, 156 orders, 236 families, 404 genera, and 621 species were identified in biofilms. At the phylum classification level, the dominant phyla in Samples 1 and 2 were similar (Figure 7). *Proteobacteria* involving a wide variety of aerobic, anaerobic, and facultative bacteria were the most dominant phylum and they accounted for 46.56 and 42.99% in Samples 1 and 2, respectively. In Sample 1, other dominant phyla mainly included *Acidobacteria* (18.23%), *Bacteroidetes* (7.71%), *Chloroflexi* (8.5%), *Patescibacteria* (5.13%), and *Firmicutes* (6.3%), while in Sample 2, it mainly included *Acidobacteria* (30.27%), *Bacteroidetes* (10.73%), *Chloroflexi* (5.9%), *Pasteurella* (3.68%), and *Firmicutes* (2.45%). Furthermore, other phyla were also detected in Samples 1 and 2, *Actinobacteriota* (2.01 and 0.53%), *Nitrospirota* (2.02 and 0.03%), and *Myxococcota* (1.67 and 0.09%).

Figure 8 shows the significance of species differences at the phylum level. After the ozone-treated solution entered the BAF, the amounts of microbial species on the filler changed. The proportions of *Acidobacteria* and *Bacteroidetes* increased significantly, and the relative abundance differences were  $-12.5$  and  $-3.01\%$ , respectively, indicating that the *Acidobacteria* and *Bacteroidetes* could adapt well and survive in an environment containing ozone. The contents of *Proteobacteria*, *Chloroflexbacteria*, *Pasteurella*, *Firmicutes*, *Actinobacteria*, *Nitrospirillum*, and *Myxococcus* in the catalytic ozonation/BAF were all lower than those in the BAF. The differences in relative abundance were 3.56, 2.6, 1.45, 3.85, 1.48, 2.0, and 1.57%, respectively, indicating that these phylum bacteria were more sensitive to ozone, but they could still tolerate a certain

**Table 2** | Relevant index of bacterial richness and diversity

Samples	Sequence number	OTUs	Shannon	Simpson	Chao1
BAF (Sample 1)	30120	760	5.2037	0.0178	772.176
O <sub>3</sub> -BAF (Sample 2)	30120	499	4.2132	0.0368	576.782

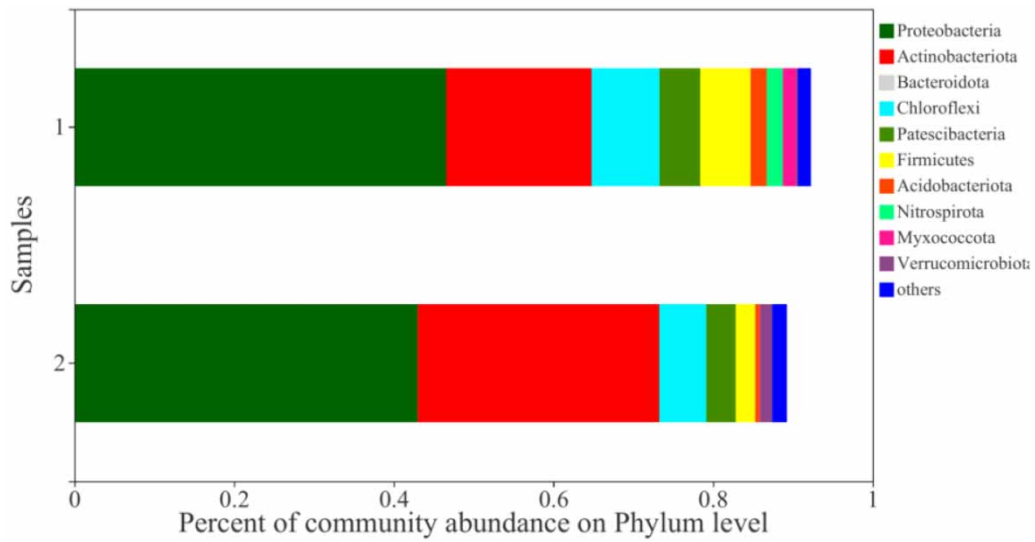


**Figure 7** | The relevant abundance of the dominant microbial community at the phylum level in two biofilm samples (Sample 1-BAF, Sample 2-catalytic ozonation/BAF).

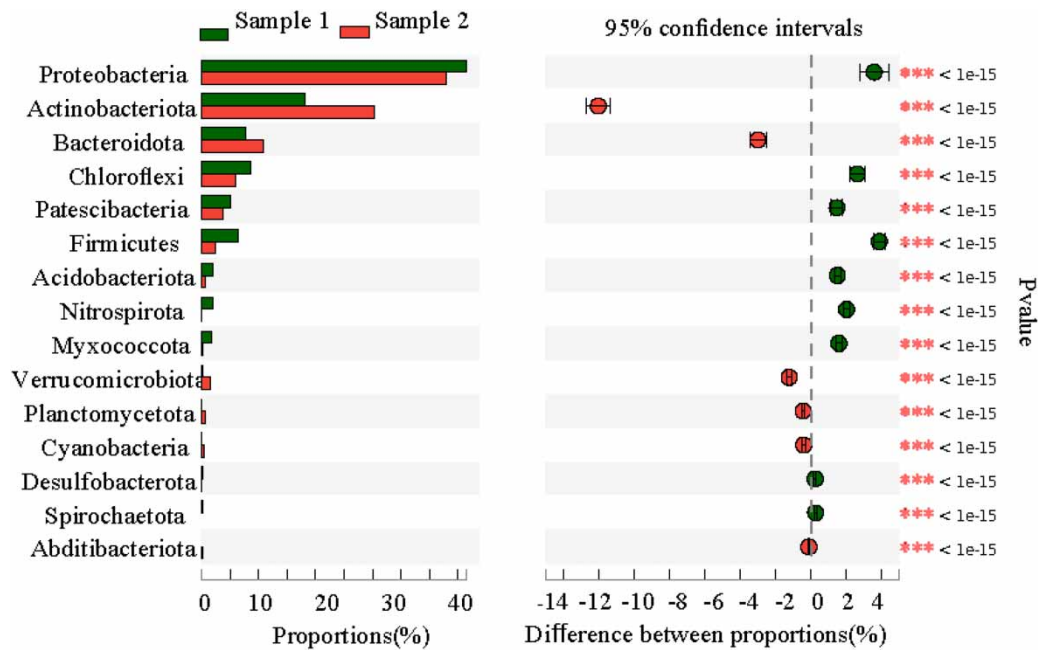


**Figure 8** | The significance of differences between species in Samples 1 and 2 at the phylum level.

amount of ozone and continue to survive in the environment with ozone. *Proteobacteria*, as a large class of bacteria, could not only degrade organic matters but also remove nitrogen and phosphorus in the biochemical process (Ding *et al.* 2018).

#### 4. CONCLUSION

A BAF equipped with homemade ceramsite was established for the efficient and stable pretreatment of secondary effluents. The surface of the filter was conducive to the attachment of microorganisms, which could effectively remove the COD and  $\text{NH}_4^+\text{-N}$  from the solution. In the BAF system, the COD ( $\text{NH}_4^+\text{-N}$ ) could decrease from 54.26 to 32.56 mg/L (decrease from

77.43 to 22.69 mg/L). Based on the experimental conditions and equipment, the COD values at different BAF heights were expressed as a function of influent COD concentration,  $\ln C/C_i = -2.53H/(QC_i^{0.622})$ . Importantly, the catalytic ozonation system could improve the biodegradability of secondary effluents, which facilitated subsequent microbial treatment. In the catalytic ozonation coupled with the BAF system, the COD and  $\text{NH}_4^+\text{-N}$  could decrease to 14.65 and 15.73 mg/L, respectively. In addition, the microbial community variation illustrated that the residual ozone in the solution could screen microorganisms and the available carbon sources in the ozone-catalyzed solution promoted thriving microbial growth. Therefore, the combined catalytic ozonation and BAF process as a promising technology can improve the overall treatment efficiency of secondary effluent.

## ACKNOWLEDGEMENTS

The financial support from the Hunan Provincial Key Research and Development Program (2022SK2068) is acknowledged.

## AUTHORS CONTRIBUTION

X.L. investigated the study, did data curation, and wrote the original draft. L.C. and J.P. edited the draft. H.L. and Y.Y. conceptualized and supervised the study, wrote the review and edited the manuscript. Z.Y. and L.Y. did the project administration.

## DATA ACCESS STATEMENT

The authors confirm that the data supporting the findings of this study are available within the article and its supplementary materials.

## DATA AVAILABILITY STATEMENT

All relevant data are included in the paper or its Supplementary Information.

## CONFLICT OF INTEREST

The authors declare there is no conflict.

## REFERENCES

- APHA 2015 *Standard Methods for the Examination of Water and Wastewater*, 23rd edn. American Public Health Association, Washington, DC.
- Bao, T., Chen, T., Wille, M.-L., Ahmadi, N. E., Rathnayake, S. I., Chen, D. & Frost, R. 2016 *Synthesis, application and evaluation of non-sintered zeolite porous filter (ZPF) as novel filter media in biological aerated filters (BAFs)*. *Journal of Environmental Chemical Engineering* **4**, 3374–3384.
- Chavez, A. M., Quinones, D. H., Rey, A., Beltran, F. J. & Alvarez, P. M. 2020 *Simulated solar photocatalytic ozonation of contaminants of emerging concern and effluent organic matter in secondary effluents by a reusable magnetic catalyst*. *Chemical Engineering Journal* **398**, 125642–125653.
- Chen, H. & Wang, J. 2021 *Catalytic ozonation for degradation of sulfamethazine using  $\text{NiCo}_2\text{O}_4$  as catalyst*. *Chemosphere* **268**, 128840–128851.
- Chen, J. J., Tu, Y. M., Shao, G. Y., Zhang, F., Zhou, Z. Y., Tian, S. C. & Ren, Z. Q. 2022 *Catalytic ozonation performance of calcium-loaded catalyst ( $\text{Ca-C}/\text{Al}_2\text{O}_3$ ) for effective treatment of high salt organic wastewater*. *Separation and Purification Technology* **301**, 121937–121950.
- Daims, H., Lebedeva, E. V., Pjevac, P., Han, P., Herbold, C., Albertsen, M., Jehmlich, N., Palatinszky, M., Vierheilig, J., Bulaev, A., Kirkegaard, R. H., von Bergen, M., Rattei, T., Bendinger, B., Nielsen, P. H. & Wagner, M. 2015 *Complete nitrification by *Nitrospira* bacteria*. *Nature* **528**, 504–509.
- Ding, P., Chu, L. & Wang, J. 2018 *Advanced treatment of petrochemical wastewater by combined ozonation and biological aerated filter*. *Environment Science and Pollution Research* **25**, 9673–9682.
- Farabegoli, G., Chiavola, A. & Rolle, E. 2009 *The biological aerated filter (BAF) as alternative treatment for domestic sewage. Optimization of plant performance*. *Journal of Hazard Material* **171**, 1126–1132.
- Friedrich, K. L., Souza, A. D. R., Fia, R., Leal, C. D., Araujo, J. C. & Siniscalchi, L. A. B. 2020 *Nitratation in pilot-scale bioreactors fed with effluent from a submerged biological aerated filter used in the treatment of dog wastewater*. *Environment Technology* 1–11. doi:10.1080/09593330.2020.1742796.
- Fu, L., Wu, C., Zuo, J., Zhou, Y. & Yang, J. 2021 *Residual ozone in microorganisms enhanced organics removal and shaped microbial community*. *Chemosphere* **278**, 130322–130332.



- Gonder, Z. B., Balcioglu, G., Vergili, I. & Kaya, Y. 2020 An integrated electrocoagulation-nanofiltration process for carwash wastewater reuse. *Chemosphere* **253**, 126713–126723.
- Jin, L., Sun, X., Ren, H. & Huang, H. 2023 Biological filtration for wastewater treatment in the 21st century: A data-driven analysis of hotspots, challenges and prospects. *Science of the Total Environment* **855**, 158951–158966.
- Li, Y., Guo, J., Li, H., Song, Y., Chen, Z., Lu, C., Han, Y. & Hou, Y. 2020 Effect of dissolved oxygen on simultaneous removal of ammonia, nitrate and phosphorus via biological aerated filter with sulfur and pyrite as composite fillers. *Bioresource Technology* **296**, 122340–122352.
- Liu, Z. Q., Tu, J., Wang, Q., Cui, Y. H., Zhang, L., Wu, X., Zhang, B. & Ma, J. 2018 Catalytic ozonation of diethyl phthalate in aqueous solution using graphite supported zinc oxide. *Separation and Purification Technology* **200**, 51–58.
- Liu, X., Li, H., Fang, Y. & Yang, Z. 2021 Heterogeneous catalytic ozonation of sulfamethazine in aqueous solution using maghemite-supported manganese oxides. *Separation and Purification Technology* **274**, 118945–118956.
- Liu, X., Yang, Z., Zhu, W., Yang, Y. & Li, H. 2022a Catalytic ozonation of chloramphenicol with manganese-copper oxides/maghemite in solution: empirical kinetics model, degradation pathway, catalytic mechanism, and antibacterial activity. *Journal of Environmental Management* **302**, 114043–114053.
- Liu, X., Zhu, W., Yang, Z., Yang, Y. & Li, H. 2022b Efficient ozone catalysis by manganese iron oxides/activated carbon for sulfamerazine degradation. *Journal of Water Process Engineering* **49**, 103050–103062.
- Mann, A. T. & Stephenson, T. 1997 Modelling biological aerated filters for wastewater treatment. *Water Research* **31**, 2443–2448.
- Nikoonahad, A., Gholizadeh, A., Ghaneian, M. T., Paseban, A., Naimi, N., Ghorbanian, M., Taghavi, M., Mohammadi, A., Abdolnabjad, A. & Moradi, B. 2022 Evaluation of a novel integrated membrane biological aerated filter for water reclamation: A practical experience. *Chemosphere* **303**, 134916.
- Parlanti, E., Wörz, K., Geoffroy, L. & Lamotte, M. 2000 Dissolved organic matter fluorescence spectroscopy as a tool to estimate biological activity in a coastal zone submitted to anthropogenic inputs. *Organic Geochemistry* **31**, 1765–1781.
- Qiu, J. L., Li, D. W., Jing, S. C., Qiu, H. & Liu, F. Q. 2022 Advanced technique of catalytic ozonation-enhanced coagulation for the efficient removal of low coagulability refractory organics from secondary effluent. *Chemosphere* **303**, 135157.
- Ren, J., Cheng, W., Wan, T., Wang, M., Meng, T. & Lv, T. 2019 Characteristics of the extracellular polymeric substance composition in an up-flow biological aerated filter reactor: The impacts of different aeration rates and filter medium heights. *Bioresource Technology* **289**, 121664.
- Satayavibul, A. & Ratanatamskul, C. 2021 A novel integrated single-stage anaerobic co-digestion and oxidation ditch-membrane bioreactor system for food waste management and building wastewater recycling. *Journal of Environment Management* **279**, 111624–111634.
- Shreve, M. J. & Brennan, R. A. 2019 Trace organic contaminant removal in six full-scale integrated fixed-film activated sludge (IFAS) systems treating municipal wastewater. *Water Research* **151**, 318–331.
- Singh, A., Srivastava, A., Saidulu, D. & Gupta, A. K. 2022 Advancements of sequencing batch reactor for industrial wastewater treatment: Major focus on modifications, critical operational parameters, and future perspectives. *Journal of Environment Management* **317**, 115305–115320.
- Su, T., Wang, Z., Zhou, K., Chen, X., Cheng, Y., Zhang, G., Wu, D. W. & Sun, S. P. 2021 Advanced treatment of secondary effluent organic matters (EfOM) from an industrial park wastewater treatment plant by Fenton oxidation combining with biological aerated filter. *Science Total Environment* **784**, 147204.
- Tang, P., Xie, W., Tiraferri, A., Zhang, Y., Zhu, J., Li, J., Lin, D., Crittenden, J. C. & Liu, B. 2021a Organics removal from shale gas wastewater by pre-oxidation combined with biologically active filtration. *Water Research* **196**, 117041–117050.
- Tang, Y., Chen, Z., Wen, Q., Yang, B. & Pan, Y. 2021b Evaluation of a hybrid process of magnetic ion-exchange resin treatment followed by ozonation in secondary effluent organic matter removal. *Science of the Total Environment* **754**, 142361–142372.
- Tang, P., Xie, W., Tian, L., Tan, B., Zhang, Y., Yang, Z., Chen, C., Zhang, W. & Liu, B. 2022 Oxidation-biotreatment-membrane combined process for external reuse of shale gas wastewater. *Separation and Purification Technology* **291**, 120920–120929.
- Ushiki, N., Fujitani, H., Shimada, Y., Morohoshi, T., Sekiguchi, Y. & Tsuneda, S. 2018 Genomic analysis of two phylogenetically distinct nitrospira species reveals their genomic plasticity and functional diversity. *Frontiers in Microbiology* **8**. doi:10.3389/fmicb.2017.02637.
- Vatankhah, H., Szczuka, A., Mitch, W. A., Almaraz, N., Brannum, J. & Bellona, C. 2019 Evaluation of enhanced ozone-biologically active filtration treatment for the removal of 1,4-dioxane and disinfection byproduct precursors from wastewater effluent. *Environment Science and Technology* **53**, 2720–2730.
- Vinoth Kumar, R., Barbosa, M. O., Ribeiro, A. R., Morales-Torres, S., Pereira, M. F. R. & Silva, A. M. T. 2020 Advanced oxidation technologies combined with direct contact membrane distillation for treatment of secondary municipal wastewater. *Process Safety and Environmental Protection* **140**, 111–123.
- Wang, S., Ma, J., Liu, B., Jiang, Y. & Zhang, H. 2008 Degradation characteristics of secondary effluent of domestic wastewater by combined process of ozonation and biofiltration. *Journal of Hazard Material* **150**, 109–114.
- Wang, Y., Lu, Y., Li, X., Zhu, G., Li, N., Han, J., Sun, L., Yang, Z. & Zeng, R. J. 2022 Light-dependent enhancement of sulfadiazine detoxification and mineralization by non-photosynthetic methanotrophs. *Water Research* **220**, 118623–118633.
- Wu, C., Gao, Z., Zhou, Y., Liu, M., Song, J. & Yu, Y. 2015 Treatment of secondary effluent from a petrochemical wastewater treatment plant by the ozonation-biological aerated filter. *Journal of Chemical Technology & Biotechnology* **90**, 543–549.
- Wu, C., Zhou, Y., Sun, X. & Fu, L. 2018 The recent development of advanced wastewater treatment by ozone and biological aerated filter. *Environment Science and Pollution Research* **25**, 8315–8329.

- Xiang, S., Han, Y., Jiang, C., Li, M., Wei, L., Fu, J. & Zhu, L. 2021 Composite biologically active filter (BAF) with zeolite, granular activated carbon, and suspended biological carrier for treating algae-laden raw water. *Journal of Water Process Engineering* **42**, 102188–102198.
- Xu, P., Han, H., Zhuang, H., Hou, B., Jia, S., Xu, C. & Wang, D. 2015 Advanced treatment of biologically pretreated coal gasification wastewater by a novel integration of heterogeneous Fenton oxidation and biological process. *Bioresource Technology* **182**, 389–392.
- Zhang, S., Zheng, J. & Chen, Z. 2014 Combination of ozonation and biological aerated filter (BAF) for bio-treated coking wastewater. *Separation and Purification Technology* **132**, 610–615.
- Zhang, L., Yue, Q., Yang, K., Zhao, P. & Gao, B. 2018 Enhanced phosphorus and ciprofloxacin removal in a modified BAF system by configuring Fe-C micro electrolysis: Investigation on pollutants removal and degradation mechanisms. *Journal of Hazard Material* **342**, 705–714.
- Zhou, H. & Xu, G. 2019 Integrated effects of temperature and COD/N on an up-flow anaerobic filter-biological aerated filter: Performance, biofilm characteristics and microbial community. *Bioresource Technology* **293**, 122004–122013.
- Zhou, H. & Xu, G. 2020 Biofilm characteristics, microbial community structure and function of an up-flow anaerobic filter-biological aerated filter (UAF-BAF) driven by COD/N ratio. *Science of the Total Environment* **708**, 134422–134432.
- Zhou, X., Zhang, Q., Sun, H. & Zhao, Q. 2019 Efficient nitrogen removal from synthetic domestic wastewater in a novel step-feed three-stage integrated anoxic/oxic biological aerated filter process through optimizing influent flow distribution ratio. *Journal of Environmental Management* **231**, 1277–1282.

First received 6 November 2022; accepted in revised form 20 March 2023. Available online 4 April 2023